

This is the peer reviewed version of the following article: Gac, J.M., Nowak, B. and Borzęcka, N.H. (2024), Cellular Automata Coupled with Two-Phase Lattice Boltzmann Model for Modeling of Kinetics of Formation and Structure of Silica-Based Sol–Gel Materials. *Adv. Eng. Mater.*, which has been published in final form at <https://doi.org/10.1002/adem.202400756>. This article may be used for non-commercial purposes in accordance with Wiley Terms and Conditions for Use of Self-Archived Versions. This article may not be enhanced, enriched or otherwise transformed into a derivative work, without express permission from Wiley or by statutory rights under applicable legislation. Copyright notices must not be removed, obscured or modified. The article must be linked to Wiley's version of record on Wiley Online Library and any embedding, framing or otherwise making available the article or pages thereof by third parties from platforms, services and websites other than Wiley Online Library must be prohibited.

## **Cellular automata coupled with two-phase Lattice Boltzmann model for modelling of kinetics of formation and structure of silica-based sol-gel materials**

*Jakub M. Gac<sup>1\*</sup>, Bartosz Nowak<sup>1</sup> and Nina H. Borzęcka<sup>1,2</sup>*

<sup>1</sup> Faculty of Chemical and Process Engineering, Warsaw University of Technology, Waryńskiego 1, 00-645 Warsaw, Poland

<sup>2</sup> Department of Aerogels and Aerogel Composites, Institute of Materials Research, German Aerospace Center (DLR), Linder Höhe, 51147 Cologne, Germany

E-mail: [jakub.gac@pw.edu.pl](mailto:jakub.gac@pw.edu.pl)

Keywords: sol-gel, numerical modeling, discrete models, kinetic of gelation

Abstract: A numerical model describing the sol-gel process on a mesoscopic scale is presented. The model is implemented as a cellular automaton (CA) based system, specifically reaction-limited aggregation merged with two-phase lattice Boltzmann method (LBM), which allows to describe the sol-gel process together with microscopic phase separation occurring during this process. The influence of model parameters on the structural properties of the resulting gel - porosity, mesoporosity and specific surface area (SSA), as well as on the kinetics of the gelation process: the shape of the kinetics curve and the structure formation time was examined. It was proposed to combine the model parameters with the composition

of the reaction mixture (the content of individual reagents and catalysts) and the process conditions.

## 1. Introduction

The sol–gel synthesis is based on a transition between two colloidal systems [1]. These are, according to the name of the method: sol – a suspension of particles in fluid, usually liquid – and gel, i.e. the structure consisting on solid skeleton built from sol particles between which permanent connections were created and in whose pores there is a liquid phase. A typical scheme of this method is as follows. In the solution containing a certain amount of precursor molecules the sol particles are formed in given conditions. These are then combining together forming the solid skeleton of gel while the remaining liquid fills its pores. The sol-gel method can be used to obtain various materials, e.g. ceramic and glass coatings, adsorbents and catalyst carriers. As a result of drying the obtained gel, it is also possible to obtain highly porous materials with a large specific surface - aerogels or xerogels [2].

Ones of the most widely investigated sol-gel systems are those arising from silica-based alcogels. These may be then become silica-based aerogels which are nowadays ones of the most popular types of aerogels [3,4]. Therefore, it is important to link the composition of the reaction mixture in which the alcogel synthesis takes place with the structure of the resulting gel as well as with the kinetics of the synthesis. For this reason, numerous experimental, as well as theoretical and numerical works were undertaken to describe the presented relationships.

Two basic types of reactions occur during the synthesis of alcogels based on organosilicon precursors [1]. The first is the hydrolysis of alkoxide groups in alkoxysilanes or organoalkoxysilanes molecules, which act as synthesis precursors. In this reaction, where the second reactant is water, these bonds are replaced by hydroxyl bonds. The next reaction is the polycondensation of hydroxyl or hydroxyl and alkoxide groups which leads to the formation of siloxane bonds between precursor molecules. As a result of these reactions, dimers and oligomers of precursors are first formed, then small particles with sizes of several nanometers (called primary particles), which in further stages combine with each other to form secondary particles. Their further aggregation (also using siloxane bonds) leads to the formation of a branched structure - gel. Its pores are filled with a mixture of water and alcohol (formed as a side effect of the hydrolysis reaction), which is why it is called alcogel. Further procedures, including replacing the solvent, carrying out a surface reaction (e.g. to hydrophobize the gel surface), and drying (supercritical or ambient pressure) depend on the desired product and will not be considered in this article.

The above description shows that the full process of gel formation from a solution containing a precursor requires a multi-scale approach, as the processes occurring on the molecular scale (hydrolysis, initial stages of polycondensation), nano- and micrometer scale (formation of primary and secondary particles) up to the macroscopic scale must be followed. allowing to take into account the properties of the entire structure with dimensions of several to several dozen millimeters or larger. In this article, however, we will focus only on a fragment of this process, namely the merging of primary particles into secondary particles and their further aggregation.

Many of the models described in the literature focus either on the description of the morphology of the gelation kinetics alone, without taking into account the morphology of the resulting structure or on the description of the morphology of the structure without taking into account the kinetics. First group of methods includes models based on reaction kinetic equations [5] or models using the Smoluchowski equation [6,7]. The second group of methods - taking into account the structure of aerogels - includes numerous numerical schemes, closely

related to the morphology of the resulting material [8]. E.g. Gaussian random field models have been applied for modeling organic non-fractal aerogels, e.g., resorcinol-formaldehyde (RF) ones [9], discrete element method (DEM)-based models are used for simulating gelation in fibrillar aerogels [10] etc. For simulation of silica aerogels with their fractal-like structure the diffusion limited particle or cluster aggregation (DLA/DLCA) method [11-13] is usually believed to be most suitable. Last time these methods are modified to take into account e.g. rotational effects, settling under gravity [14] and thus allowing to some extent describe, in addition to the structure itself, also the kinetics of the gelation process. Another modification of this group of models is the inclusion of the probability of a particle merging with a cluster or two clusters being less than one that means not all the collisions result in aggregation. The DLA/DLCA method modified in this way is called reaction-limited (cluster-)aggregation (RLA/RLCA) [15-17]. However, the model formulated in this way still did not take into account a phenomenon that may have a significant impact on the morphology and kinetics of the formation of gel structures, namely microscopic phase separation. This phenomenon is a direct result of the limited miscibility of the two reagents involved in the hydrolysis reaction - the precursor and water. As a result, two phases are created in the system - one rich in water, the other - in the precursor. Gelation as a reaction between precursor molecules takes place, of course, mainly in the second phase, which can be called the gelling phase. It is therefore expected that the size and shape of the areas occupied by individual phases will influence the morphology of the resulting structures and the speed of their formation. To take this effect into account, a model based on the DLA or RLA algorithm should be supplemented with a description of microscopic phase separation.

Modeling the dynamics of phase separation can be implemented using various widely used methods, the most popular of which are the finite volume method (FVM) [18-20] and finite element method (FEM) [21-23]. However, both groups of methods mentioned above provide the best results for macroscopic systems, i.e. those where the characteristic sizes of the system significantly (by several orders of magnitude) exceed the sizes of the molecules [19]. If we are interested in the dynamics of gelation at the mesoscopic level, i.e. when we consider objects - primary particles - with sizes only two or three times larger than the size of the molecules, a better approach is to use algorithms based on the lattice gas method [24]. In this group of algorithms, the lattice-Boltzmann method (LBM) [25,26] has gained the greatest popularity, which is based on solving a triple discretized (in the domain of time, space and velocity) form of the Boltzmann kinetic equation. This method has been successfully applied to solution of such problems as flow in canals with more or less complicated geometry [27], shallow water flow [28,29] or flow of non-newtonian fluids [30]. There are also algorithms that allow the use of the LBM formalism to describe multiphase flows [31,32]. We can distinguish models such as Shan–Chen multiphase model [33-34], free energy based approach [35-36] and two-color model, known also as color-gradient model [37,38]. The latter turned out to be the most convenient and effective in the case of two-phase flows for fluids with slightly different densities and will therefore be used in this work.

## 2. Methods

### 2.1. Model formulation

The numerical model presented in this work is a combination of the Boltzmann lattice gas model and a model based on the cellular automata method, or more precisely - on the DLA/RLA approximation.

The two-phase version of the LBM simulates the separation of the mixture into phases - it is an approximation of the observed phenomenon of microscopic phase separation. The classical LBM [25,26] has been elaborated to solve the kinetic Boltzmann equation for the particle distribution function (PDF)  $f(\mathbf{x}, \mathbf{v}, t)$  which is defined as a probability density of finding a portion of fluid in given space  $(\mathbf{x}, \mathbf{x} + d\mathbf{x})$  at given time and with given velocity  $(\mathbf{v}, \mathbf{v} + d\mathbf{v})$ . In LBM description all three values are discretized, i.e. instead of continuous function as mentioned above we have its discrete analogue  $f_i(\mathbf{x}, t)$ , where subscript  $i$  denotes the number of discrete velocity direction. This number is dependent on mesh geometry and for 3D mesh it is typically between 15 and 27 direction (one of the represents the zeroth vector) [39].

The evolution of the PDF is described by two successive steps: propagation and collision, which mimics the evolution of real particles in the fluid. The dynamics of PDF in classical LBM is realized as follows:

$$f_i(\mathbf{x} + \mathbf{c}, t + 1) = f_i(\mathbf{x}, t) + \Omega(\mathbf{x}, t) \quad (1)$$

where  $\Omega(\mathbf{x}, t)$  denotes the so-called collision term and is the discrete analogue of collision integral in kinetic Boltzmann equation. According to the most common Bhatnagar-Gross-Krook (BGK) [40,41] formulation it is described as follows:

$$\Omega(\mathbf{x}, t) = \frac{1}{\tau} (f_i(\mathbf{x}, t) - f_i^{eq}(\mathbf{x}, t)) \quad (2)$$

Where  $f_i^{eq}(\mathbf{x}, t)$  denotes the equilibrium value of PDF and is given as [26]:

$$f_i^{eq}(\mathbf{x}, t) = \rho w_i \left( 1 + 3\mathbf{c}_i \cdot \mathbf{u} + \frac{9}{2}(\mathbf{c}_i \cdot \mathbf{u})^2 - \frac{3}{2}\mathbf{u}^2 \right) \quad (3)$$

In above  $\rho$  means lattice gas density (not to be confused with the actual density of the fluid),  $\mathbf{c}_i$  is the  $i$ -th vector of lattice and  $w_i$  -  $i$ -th weight of lattice (the two last are dependent on mesh geometry and their values may be found in some reviews papers on LBM) and  $\mathbf{u}$  is the fluid velocity at point  $\mathbf{x}$ . The velocity field can be determined using the dependency:

$$\mathbf{u} = \frac{\sum_i \mathbf{c}_i f_i(\mathbf{x}, t)}{\sum_i f_i(\mathbf{x}, t)} \quad (4)$$

In our model the LBM formalism will be used for description of phase separation during the gelation process. Thus the multiphase LBM has been introduced. In present work we use so-called two-color LBM method [42, 43]. In two-color LBM model the modified PDF is used in form  $f_i^k(\mathbf{x}, t)$  where superscript  $k = r$  or  $b$  denotes the 'color' ('red' or 'blue'). Both of the functions evolve according to eq. (1):

$$f_i^k(\mathbf{x} + \mathbf{c}, t + 1) = f_i^k(\mathbf{x}, t) + \Omega_i^k(\mathbf{x}, t) \quad (1a)$$

but the collision operator consists of two terms:

$$\Omega_i^k(\mathbf{x}, t) = \left( \Omega_i^k(\mathbf{x}, t) \right)^{(1)} + \left( \Omega_i^k(\mathbf{x}, t) \right)^{(2)} \quad (5)$$

The term  $\left( \Omega_i^k(\mathbf{x}, t) \right)^{(1)}$  is given by means of (2) and the second term is given in form:

$$\left( \Omega_i^k(\mathbf{x}, t) \right)^{(2)} = \frac{A_k}{2} |\mathbf{F}| \left[ W_i \frac{(\mathbf{F} \cdot \mathbf{c}_i)}{|\mathbf{F}|^2} - B_i \right] \quad (6)$$

where  $\mathbf{F}$  is a local gradient of color,  $W_i$  and  $B_i$  are the constant values, given in [44] and  $A_k$  is the value proportional to the surface tension coefficient; further will be called as lattice surface tension coefficient so as not to be confused with physical surface tension coefficient. It has been shown that these two parameters are joined together by the formula [45]:

$$\sigma = 1.3258 A_k \tau_k + 0.0083 \quad (7)$$

To complete the single time-step, the recoloring of the particles is applied. The recoloring is the procedure, which ensures the conservation of the total densities of both fluids and total momentum at each site. In this paper, we apply the recoloring scheme proposed in [20]. It is much less complicated than that applied in the work [21] and more stable than that used in

[24]. The discussion concerning stability of various recoloring schemes can be found in [20]. According to this method, we compute the new values of PDF's using the equations:

$$f_i^{r,new} = \frac{\rho_r}{\rho_r + \rho_b} (f_i^r + f_i^b) + \beta \left( \frac{\rho_r \rho_b}{\rho_r + \rho_b} \right)^2 \cos \phi_i \quad (28)$$

$$f_i^{b,new} = \frac{\rho_b}{\rho_r + \rho_b} (f_i^r + f_i^b) - \beta \left( \frac{\rho_r \rho_b}{\rho_r + \rho_b} \right)^2 \cos \phi_i \quad (29)$$

where  $\phi_i$  denotes the angle between the color gradient and the direction of i-th vector  $\mathbf{c}_i$  and  $\beta$  is the value that controls the thickness of the interface.

After completing this step, the time is increased and the new propagation step is made.

Within one of these phases, let's call it the gelling phase, the structure is simulated in accordance with the off-lattice DLA/RLA [17] algorithm as presented in work [46]. In this algorithm, the particles subject to diffusion are identified as primary particles of the gel. We distinguish two types of particles: seed particles which may be identified as the local beginnings of the structure and walker particles which are responsible for the expansion of the structure. The clusters are formed by attaching the walker particles to seeds or to already existing clusters. Unlike the work [46], the diffusion of both types of particles takes place on-lattice, which means that at each time step the particle jumps to one of the neighboring nodes. Clusters are also subject to diffusion but it is slower than in the case of walker particles. In the case of the on-lattice formulation presented here, this means that the probability of all particles constituting a cluster synchronously jumping to neighboring nodes (and thus shifting the entire cluster by the length of the lattice edge) is less than unity. Moreover, for larger cluster sizes, the hop probability is lower.

An additional limitation on the movement of particles and clusters is the assumption that they cannot leave the gelling phase. Therefore, if a particle or cluster were to cross the phase boundary as a result of diffusive movement, this movement is automatically rejected and the direction is selected again so that the particle/cluster remains within the gelling phase. On the other hand, the presence of aggregates influences the phase size dynamics. It is assumed that the clusters are perfectly wetted by the gelling phase (contact angle equal to zero), which is an additional condition for the movement of the phase boundary.

## 2.2. Simulation process and results preparation

The numerical simulations were as follows. For the initial 200 time steps, only the changes described by LBM occurred in the system, without taking into account particle diffusion and combining. After this time, the DLA/RLA mechanism was turned on and the actual gelation phase began. It lasted for 15,000 time steps, or until all particles were combined into a structure (structure disintegration, particle detachment, etc. were not taken into account).

Quantitative analysis included:

- a. determination of total porosity and mesoporosity
- b. determination of the specific surface of the resulting structure.
- c. determination of the kinetic curve, i.e. the number of particles included in the structure (constituting clusters)
- d. determination of time of structure formation.

Total porosity was determined as the ratio of the number of cells not included in the cluster. The mesoporosity is determined as follows. For each empty site in the lattice, a sphere surrounding it with a radius equal to three edge lengths of the lattice is considered. If at least half of the sites in this sphere are empty, including at least half of the sites directly adjacent to

the site in question - this site is treated as belonging to the mesopore. Mesoporosity is then calculated as the ratio of the number of sites classified as mesopores to the number of sites in the entire domain. For obvious reasons, this is less - or at least not more - than the porosity defined above.

The specific surface area (SSA) is defined as a number of particle walls constituting the cluster(s) that are simultaneously adjacent to empty cells. From this we can see that the upper limit SSA value can be equal to  $6 \cdot (N_w + N_s) / L_x \cdot L_y \cdot L_z$

The kinetic curve is determined as the total number of particles included in all clusters (defined as a measure of the gel mass - i.e. simply dimensionless mass) in successive time steps. Based on the kinetic curve, the structure formation time is determined as the number of time steps from the start of the DLA/RLA simulation until the mass of the cluster(s) reaches a value equal to 85% of the total number of walkers and seeds.

### 3. Results of computation

The description presented in the "Methods" Sec. shows that the presented model has five parameters that can be changed to describe a specific case. These parameters are: (i) the number of seeds particles, (ii) the number of walker particles, (iii) the volume fraction of the gelling phase, (iv) the lattice surface tension coefficient and (v) the probability of including diffusing particles (hereinafter referred to as RLA probability). To analyze the impact of individual parameters on the structure of the resulting gels, it is worth first considering the range of variability of the values of individual parameters.

As for the number of particles (total number of seeds and walkers), it must certainly be smaller than the number of network nodes so that diffusion is possible. Calculations show that when the number of particles exceeds one third of the number of nodes, their ability to move is severely limited and within a few steps one large cluster (gel) is formed. This value also depends on the volume fraction of the gelling phase (see below) - for lower values of this fraction the maximum number of particles is also smaller. The lower limit results from the fact that if the number of particles is too small, very small clusters will be formed that will not be able to combine into one larger cluster. As for the volume fraction of the gelling phase, it can range from 0 to 1. However, if it is too small, the diffusive movement of particles will again be greatly hampered. The probability of particle attachment ranges from 0 to 1 (a value of 1 means diffusion limited aggregation). Finally, the value of the lattice surface tension coefficient is limited from above by a value of 0.01, above which the algorithm loses numerical stability.

#### 3.1. Structure description

The analysis of the final states obtained with different sets of parameters allows the identification of three basic types of structures, which are presented in Fig. 1. The first type is a structure with relatively low porosity (below 0.8) and very low mesoporosity (less than 0.25). and high SSA (more than 0.55). This structure is presented in Fig. 1A. This type of structure has a form of a compact monolith, but with many small pores inside. The opposite type is characterized by high porosity (over 0.95) and mesoporosity (over 0.8) followed by low SSA (below 0.18). In this structure we observe the spherical – or close to spherical - aggregates of primary particles which together form a branched structure (Fig. 1B). Finally, an intermediate structure is also observed, in which we can also distinguish nearly-spherical aggregates of primary particles but connected in a more compact way as it has been presented in Fig. 1C.

In addition to the above, there are also cases where large clusters are not formed, instead the final system consists of single seed particles and small clusters that do not agglomerate for a

very long time (until the end of the simulation). Such a case can be considered analogous to the formation of precipitates during a synthesis reaction. Precipitates are formed when the mass fraction of the precursor is very small.

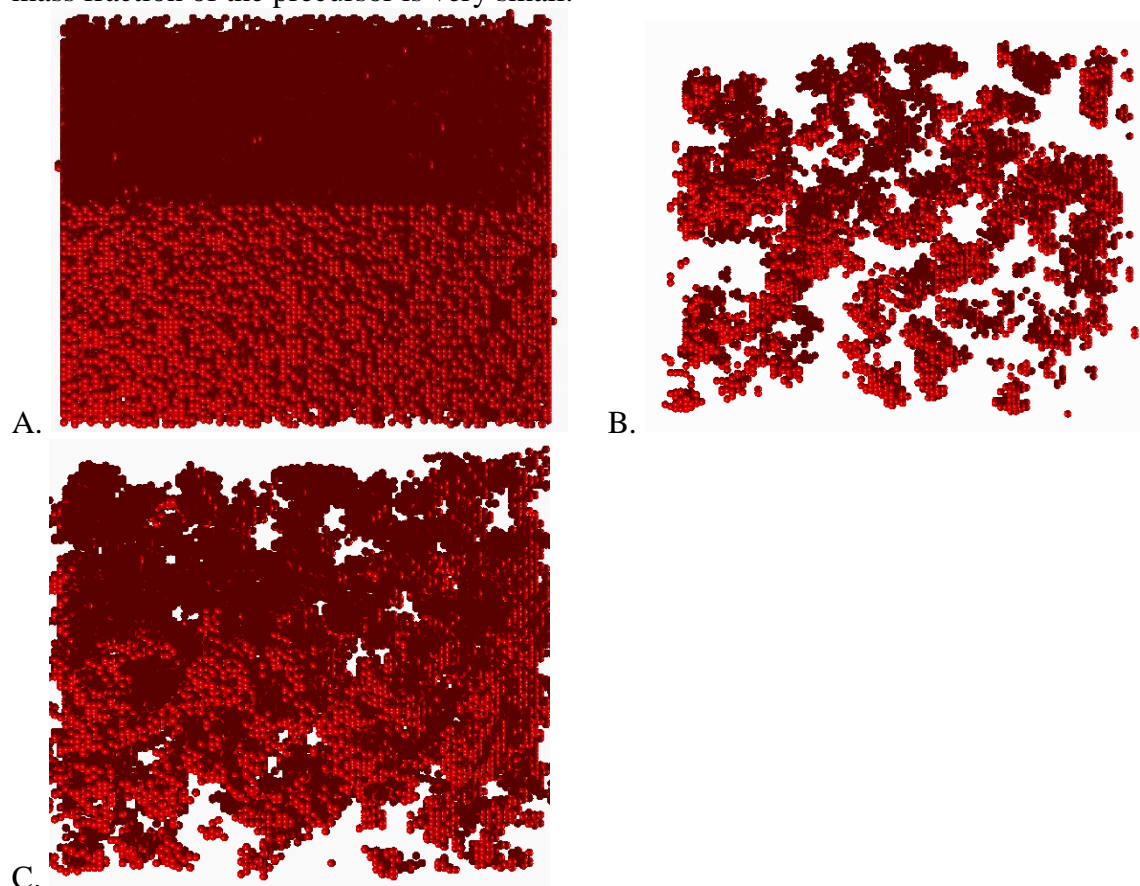


**Figure 1.** Exemplary snapshots of three types of structures obtained in simulations (see text for details).

Fig. 2 shows the interplay of porosity and mesoporosity (for about 70 samples, those which have not formed the cluster were omitted). As you can see, these values are quite strongly linearly correlated. Moreover, on the presented graph it is possible to distinguish three groups of points that correspond to the morphologies described above. It also turns out that, according to the description presented, each group is characterized by a significantly different SSA value.

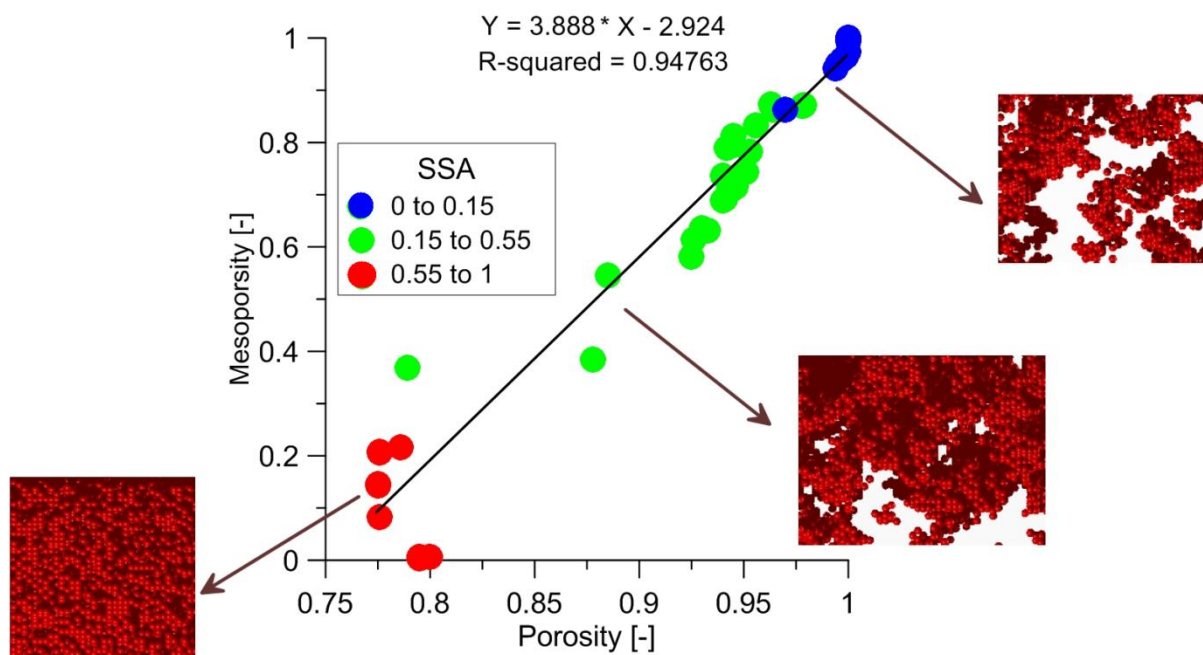


**Figure 2.** The dependence between porosity, mesoporosity, SSA and structure morphology of numerically obtained gels.

The above structures can be classified according to the classification proposed by Nakanishi's team [47, 48]. The first structure - with low porosity and a very small number of mesopores and a relatively large specific surface area - can be described as a nanoporous structure. The second structure refers to the morphology of "particle aggregates", and the third - transitional, visually resembles the co-continuous structure. Nakanishi associated these structures with the mechanism of phase separation: the morphology of particle aggregates is related to the mechanism of nucleation and growth of the gelling phase, the nanoporous morphology corresponds to the spinodal decomposition mechanism, while the co-continuous morphology is a transitional structure (Nakanishi refers to it as "frozen"). The issue of the phase separation mechanism in the discussed model will be discussed below.

Porosity - and with it mesoporosity and SSA - depends most strongly on three of the five mentioned model parameters: the number of walkers, the volume fraction of the gelling phase and the RLA probability. The dependence of porosity on the number of walkers is generally strictly decreasing, which results directly from the geometry of the model formulated in this way. As it can be seen in Fig. 4A, this dependence may be described – with  $R^2 > 0.9$  – by means of linear equation. Simply put, the more particles there are in the system, the larger the clusters are formed and the fewer empty cells remain. The dependence on other parameters is slightly less clear. The dependence of porosity on the volume fraction of the gelling phase and the RLA probability is shown in Fig. 3B. It can be seen here that the highest porosity is achieved for the lowest fraction of the gelling phase, which is obvious if we consider that only in this phase gel is formed (cells belonging to the second phase will form pores by the very nature of the model). Particularly high porosity values are obtained here for two extreme values of the RLA probability - very small and 1. The first case - a very low RLA probability - means the formation of small compact aggregates, between which there is a lot of empty space - pores. In turn, an RLA probability of 1 means that we are in fact dealing with a DLA mechanism, which leads to the formation of highly developed but loose aggregates.

The lowest porosity occurs for the fraction of the gelling phase close to 0.5 and small values of RLA probabilities. Under these conditions, compact aggregates are formed, but due to the limited volume of the gelling phase, their mutual arrangement is also quite compact. As we

increase the volume of the gelling phase, the larger space available for aggregation promotes the formation of slightly looser structures and, therefore, greater porosity - although not as high as for the low value of the gelling phase fraction.

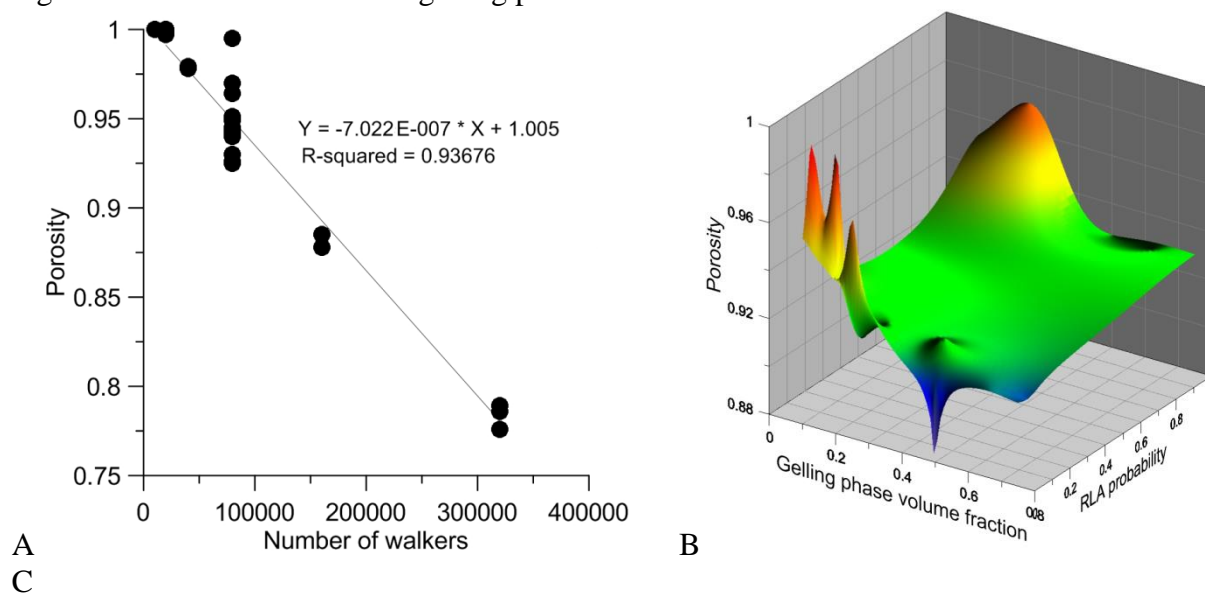


**Figure 3.** Porosity of final structure as a function of (A) number of walkers and (B) gelling phase volume fraction and RLA probability.

### 3.2. Kinetics of aggregate formation

The kinetics of aggregate formation were examined by analyzing the shape of the curve describing the dependence of the total mass of aggregates on time and the time of structure formation in accordance with the information in Sec. XX. The shape of the kinetic curve for each case in which cluster formation occurred was sigmoidal: after an initial period of phase separation, there was a sharp increase, then the growth rate decreased, asymptotically reaching the final mass value. In order to analyze the dependence of the shape of the curve on individual parameters, their base values were determined, listed in Table 1. These were average values in relation to the minimum and maximum values presented above. Then the value of one of the parameters was changed and the curves thus obtained were compared.

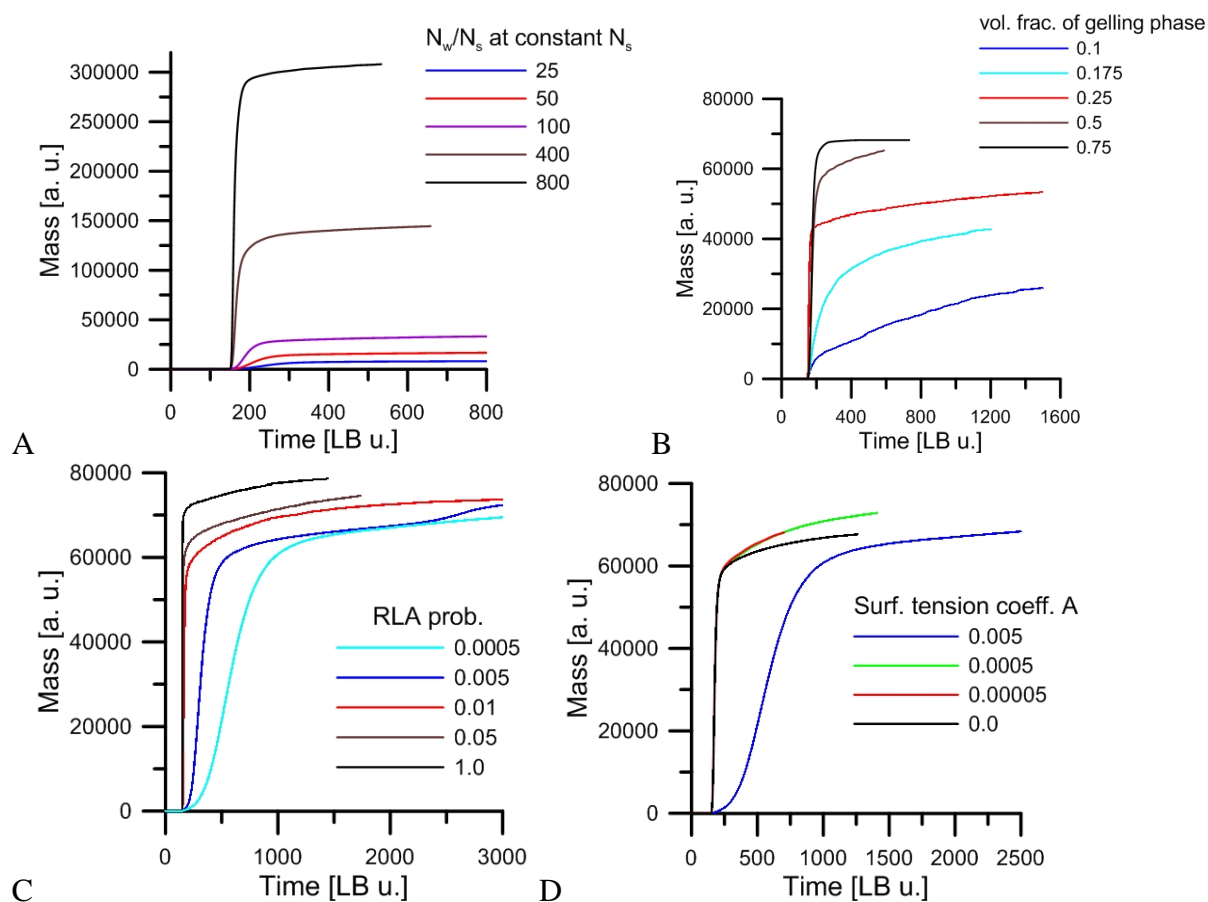
**Table 1.** Base values of kinetics simulation

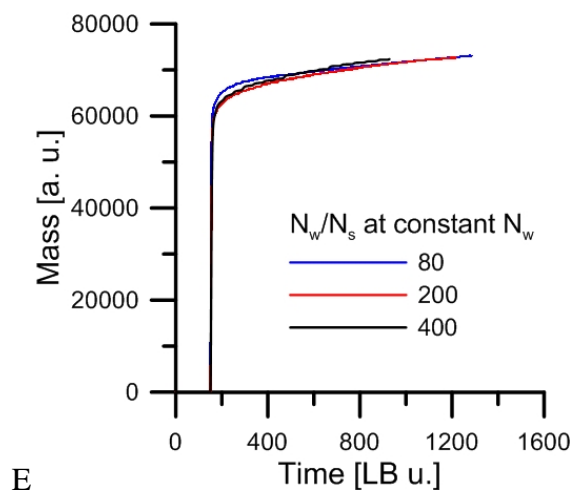
Quantity	Value
Number of walkers	80000
Number of seeds	400
Volume fraction of gelling phase	0.5
Lattice coefficient of surface tension	0.005
Probability RLA	0.05

The main parameter influencing the kinetics of condensation is of course the walker number. In Fig. 4A there are presented a few kinetic curves for different values of walker number (described as different walkers to seeds ratio number at constant number of seeds). The first thing which is observed is of course the fact that the final value of mass is different (and equal approximately to the sum of numbers of walkers and seeds).

When consider the dependence of kinetic curve on gelling phase volume fraction (Fig. 4B) we observe the following pattern. When the volume fraction is equal to or exceeds 0.25 the time of cluster formation is very short and the gel mass shortly achieves the final (or close to final) value. These are in general different for various values of gelling phase fraction though the same number of walkers and seeds. The reason is that some walkers may become trapped in isolated "droplets" of the gelling phase. These particles will not take part in the formation of the gel and will not attach to the structure. The increase in the mass of structures is different at lower values of the volume fraction of the gelling phase. In this case, an initial surge may be observed, but this is followed not by a plateau but by further gradual, slower growth. This is due to the fact that walkers initially enclosed in isolated "droplets" gain the opportunity to be incorporated into the structure when these drops combine with drops that already contain a cluster. In such a situation, the time needed to create the aggregate is very long.

Fig. 4C shows the kinetic curves for different values of the RLA parameters. In this case, we see that as this probability increases, the curve becomes steeper. The time needed to create the structure is also shortened. In the case of dependence on the number of walker particles, the shape of the curves is similar, although of course the value of the final mass of the structure is different.





E

**Figure 4.** Kinetics curves of gel formation for different values of (A) walkers to seeds number ratio for constant number of seeds, (B) volume fraction of gelling phase, (C) RLA probability, (D) lattice surface tension coefficient and (E) walkers to seeds number ratio for constant number of walkers.

The analysis of the dependence of the structure formation time on both the fraction of the gelling phase and the RLA probability (Fig. 5) shows that for each value of the RLA probability there is a minimum of this time at the fraction of the gelling phase equal to 0.5. When the RLA probability is much smaller than 1, increasing the fraction of the gelling phase leads to a relatively small increase in the structure formation time, which is due to the increase in the average number of steps needed to "hit" the walker particle into the cluster (the result of a larger area available for particle and cluster diffusion). However, reducing the fraction of the gelling phase leads to a significant extension of this time for the reasons mentioned above. For low values of the RLA probability and low fractions of the gelling phase, the structure formation time has the highest values. The lowest values are observed for the RLA probability equal to one and the gelling phase fraction equal to 0.5. The latter is also influenced by the factors already mentioned - the optimal area for the diffusion of particles, allowing them to "meet" the cluster quite quickly, and the immediate attachment of particles to the cluster.

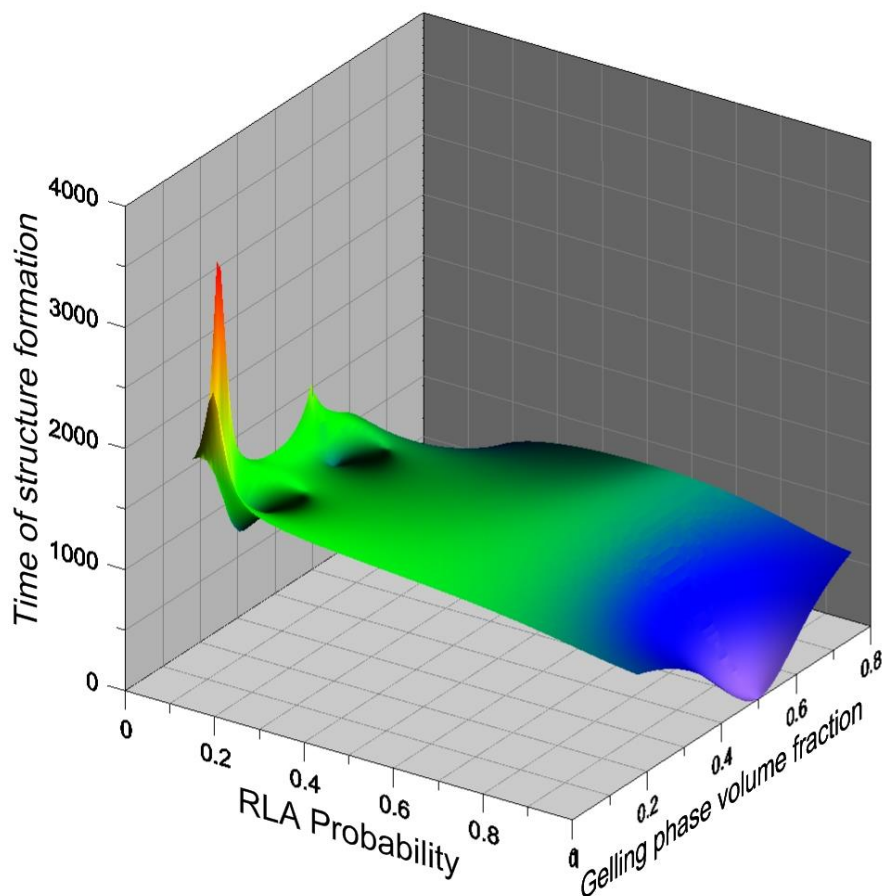


**Figure 5.** Time of structure formation as a function of RLA probability and gelling phase volume fraction.

The dependence of the form of the kinetic curve on the lattice coefficient of surface tension (Fig. 4D) is more complex. At values lower than 0.005, the curves practically coincide, while at higher values the mass growth rate slows down significantly. Finally, the number of seed particles does not affect the shape of the kinetic curve at all as seen in Fig. 4E. For values of seeds from 200 to 1000 (that means the walker to seeds ratio between 80 and 400 for fixed walkers ratio) the curves practically coincide.

The fact that the above-mentioned model parameters have a specific impact on the structure of the emerging gel and the kinetics of its formation result in specific connections between structural properties (porosity) and kinetic properties (structure formation time). Fig. 6 shows these relationships, Fig. 6A shows that the structure formation time is generally longer for structures with higher porosity. This is due to the fact that the same model parameters that influence the increase in porosity (low RLA probability value and low fraction of the gelling phase) also influence the extension of the structure formation time. This regularity is even more visible in the case of the dependence of this time on mesoporosity. Of course, this is not a clear-cut relationship, because there are as many as five parameters influencing both parameters (four if we ignore the number of seeds, which practically does not affect any of these values), which greatly complicates their mutual interdependence.

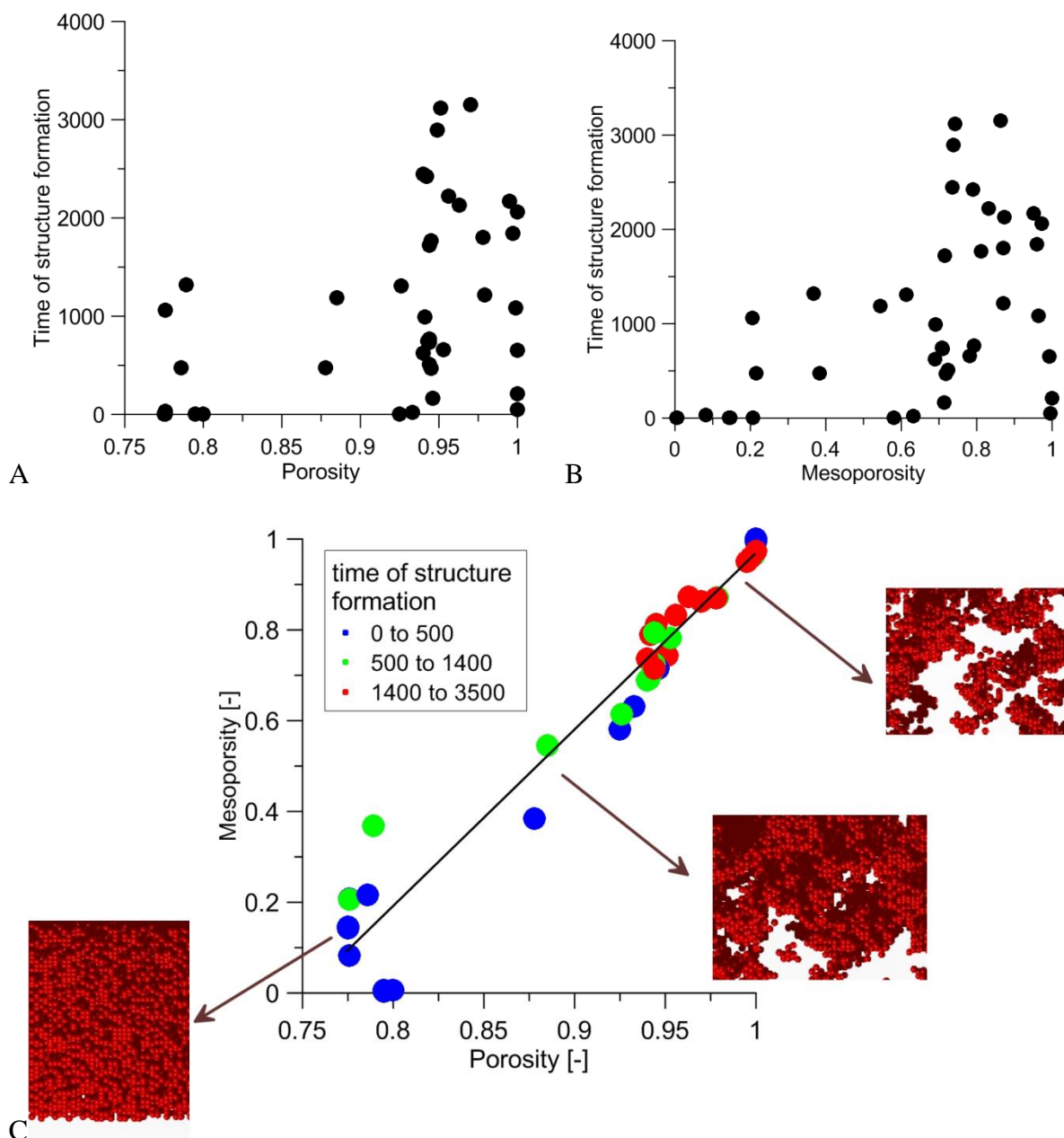


**Figure 6.** Time of structure formation for structures with different (A) porosity and (B) mesoporosity and (C) the joint dependence between porosity, mesoporosity and time of structure formation.

The plot in Fig. 6C confirms this correlation. It is visible, however, that the time of creating a structure with a porosity close to 0.95 may be within very wide limits - in this region there are times both lower than 500 and above 1400. Attention is also drawn to single points corresponding to low times for porosity and mesoporosity close to 1. There are structures for which the RLA probability was 1.

#### 4. Discussion and conclusion

The paper presented a proposal for a numerical model to describe the sol-gel process on a mesoscopic scale, i.e. taking into account the fusion of primary particles into secondary particles and then into the final structure of the resulting gel. The described approach takes

into account both the (diffusive) movement and agglomeration of primary particles, as well as the parallel phenomenon of microscopic phase separation.

In order for the presented model to be used in the future to predict the impact of the reaction mixture on the actual properties of the obtained gels and their kinetics, the model parameters should be linked to the mixture parameters. The number of all particles - or the number of walker particles (since the number of seeds is typically much smaller and, as shown, does not significantly affect both the structure parameters and the kinetics of its formation) is certainly related to the precursor concentration. The nearly linear, decreasing dependence of porosity on the walkers number – i.e. precursor concentration – is confirmed by some experimental results [49, 50]. The modeling results also show that the structure formation time is a decreasing function of the number of walkers. However, if we strictly equate the number of walkers with the precursor concentration, the experimental results do not confirm this conclusion. The gelation time measured in various systems reaches its minimum value for a certain precursor concentration, and more precisely for the water to precursor concentration ratio [51, 52]. This may be due to the fact that the precursor concentration should influence not only the number of walkers, but also the volume fraction of the gelling phase. Indeed, if the precursor concentration is very low, the volume fraction of the gelling phase will also be small, and under certain conditions phase separation may not occur at all. This means that the mentioned parameters - the number of walkers and the volume fraction of the gelling phase - are not completely independent and some of their combinations (e.g. a small number of walkers and a high value of the mentioned volume fraction) cannot be implemented in real conditions.

Another parameter that affects the value of the volume fraction of the gelling phase is the water concentration in the reaction mixture. This concentration, together with the concentration of the surfactant and/or solvent, e.g. alcohol (if present in the solution), also affects the value of the lattice surface tension coefficient (which is directly related to the physical surface tension coefficient). It is expected that increasing the surfactant concentration will generally lead to a decrease in the surface tension coefficient. In turn, increasing the solvent concentration may lead to mutual miscibility of both phases. The gelling phase will then formally cover the entire computational domain, and the lattice surface tension coefficient will become zero. This situation will lead to the formation of particle aggregate structures (for the cases analyzed in this work, all variants for which the lattice surface tension coefficient was equal to zero resulted in the formation of a structure with a porosity above 0.95), which is consistent with the experimental results [47]. It is also known from experiments that macroscopic phase separation should occur under these conditions [5], which however is impossible to reconstruct using the mesoscopic model we present here.

Finally, the RLA probability, and therefore the probability of adding further primary particles to the emerging structure, depends on the activation energy, which can be related to the catalyst concentration. In our previous work [17] we showed that this probability is directly dependent on the concentration ratio of the hydrolysis catalyst to the precursor and increases with this ratio. Moreover, it has been shown that this probability is an increasing function of the process temperature. It should be assumed that in the current, extended model, the same factors will influence the value of this probability.

Summarizing the above considerations, it should be stated that the numerical model presented in this work provides a good basis for predicting the properties and kinetics of gel formation in the mesoscopic scale. The issue of relating model parameters to the composition of the reaction mixture and synthesis conditions requires further work.

## Acknowledgements

This work was funded by POB Technologie Materiałowe of Warsaw University of Technology within the Excellence Initiative: Research University (IDUB) programme.

Received: ((will be filled in by the editorial staff))

Revised: ((will be filled in by the editorial staff))

Published online: ((will be filled in by the editorial staff))

## References

- [1] Brinker, C. J.; Scherer, G. W. CHAPTER 3 - Hydrolysis and Condensation II: Silicates. In *Sol-Gel Science*; Brinker, C. J., Scherer, G. W., Eds.; Academic Press: San Diego, **1990**; pp 96–233.
- [2] Innocenzi, P. *The Sol to Gel Transition*; SpringerBriefs in Materials; Springer International Publishing: Cham, 2016.
- [3] Gurav, J. L.; Jung, I.-K.; Park, H.-H.; Kang, E. S.; Nadargi, D. Y. *J. Nanomaterials* **2010**, *2010*, 23:1-23:11.
- [4] Rashid, A. B.; Shishir, S. I.; Mahfuz, Md. A.; Hossain, Md. T.; Hoque, M. E. *Particle & Particle Systems Characterization* **2023**, *40*, 2200186.
- [5] Borzęcka, N. H.; Nowak, B.; Gac, J. M.; Głaz, T.; Bojarska, M. *Journal of Non-Crystalline Solids* **2020**, *547*, 120310.
- [6] Jiang, Y.; Gang, H.; BenKun, M. *Phys. Rev. B* **1990**, *41* (13), 9424–9429.
- [7] Ratke, L.; Hajduk, A. *Gels* **2015**, *1* (2), 276–290.
- [8] Rege, A. *Advanced Engineering Materials* **2023**, *25* (1), 2201097.
- [9] Roberts, A. P. *Phys. Rev. E* **1997**, *55* (2), R1286–R1289.
- [10] Depta, P. N.; Gurikov, P.; Schroeter, B.; Forgács, A.; Kalmár, J.; Paul, G.; Marchese, L.; Heinrich, S.; Dosta, M. *J. Chem. Inf. Model.* **2022**, *62* (1), 49–70.
- [11] Hsieh, K.; Lallet, F.; Olivi-Tran, N. *Fractals* **2008**, *16* (04), 361–365.
- [12] Abdusalamov, R.; Scherdel, C.; Itskov, M.; Milow, B.; Reichenauer, G.; Rege, A. *J. Phys. Chem. B* **2021**, *125* (7), 1944–1950..
- [13] Rahmani, A.; Benoit, C.; Jullien, R.; Poussigue, G.; Sakout, A. *J. Phys.: Condens. Matter* **1996**, *8* (30), 5555.
- [14] Polimeno, M.; Kim, C.; Blanchette, F. *ACS Omega* **2022**, *7* (45), 40826–40835.
- [15] Wijnen, P. W. J. G.; Beelen, T. P. M.; Rummens, C. P. J.; van Santen, R. A. *Journal of Non-Crystalline Solids* **1991**, *136* (1), 119–125.
- [16] Borzęcka, N. H.; Nowak, B.; Pakuła, R.; Przewodzki, R.; Gac, J. M. *Gels* **2021**, *7* (2), 50.

- [17] Borzęcka, N. H.; Nowak, B.; Pakuła, R.; Przewodzki, R.; Gac, J. M. *International Journal of Molecular Sciences* **2023**, *24* (3), 1999.
- [18] Blazek, J. Chapter 4 - Structured Finite Volume Schemes. In *Computational Fluid Dynamics: Principles and Applications (Second Edition)*; Blazek, J., Ed.; Elsevier Science: Oxford, **2005**; pp 77–129.
- [19] Versteeg, H. K.; Malalasekera, W. *An Introduction to Computational Fluid Dynamics: The Finite Volume Method*; Pearson Education, 2007.
- [20] Moukalled, F.; Mangani, L.; Darwish, M. The Finite Volume Method. In *The Finite Volume Method in Computational Fluid Dynamics: An Advanced Introduction with OpenFOAM® and Matlab*; Moukalled, F., Mangani, L., Darwish, M., Eds.; Springer International Publishing: Cham, **2016**; pp 103–135.
- [21] Huyakorn, P. S., K. Nilkuha, *Appl. Math. Model.*, **1979**, *3*, 7–17.
- [22] Kaluarachchi, J. J.; Parker, J. C. *Water Resources Research* **1989**, *25* (1), 43–54.
- [23] Ihueze, C. C. *Journal of Minerals and Materials Characterization and Engineering* **2010**, *9* (5), 427–454.
- [24] Rothman, D. H.; Zaleski, S. *Lattice-Gas Cellular Automata: Simple Models of Complex Hydrodynamics*; Collection Alea-Saclay: Monographs and Texts in Statistical Physics; Cambridge University Press: Cambridge, **1997**.
- [25] McNamara, G. R.; Zanetti, G. *Phys. Rev. Lett.* **1988**, *61* (20), 2332–2335.
- [26] Chen, S.; Doolen, G. D *Annual Review of Fluid Mechanics* **1998**, *30*, 329–364.
- [27] Psihogios, J.; Kainourgiakis, M. E.; Yiotis, A. G.; Papaioannou, A. Th.; Stubos, A. K. *Transp Porous Med* **2007**, *70* (2), 279–292.
- [28] Zhou, J. G. *Computer Methods in Applied Mechanics and Engineering* **2002**, *191* (32), 3527–3539.
- [29] Ru, Z.; Liu, H.; Tu, G.; Xing, L.; Wu, X.; Ding, Y.; Shao, D. *International Journal for Numerical Methods in Fluids* **2022**, *94* (4), 295–315.
- [30] Wang, C.-H.; Ho, J.-R. *Computers & Mathematics with Applications* **2011**, *62* (1), 75–86.
- [31] Grunau, D.; Chen, S.; Eggert, K. A Lattice Boltzmann Model for Multiphase Fluid Flows. *Physics of Fluids A: Fluid Dynamics* **1993**, *5* (10), 2557–2562.
- [32] Sudhakar, T.; Das, A. K. Evolution of Multiphase Lattice Boltzmann Method: A Review. *J. Inst. Eng. India Ser. C* **2020**, *101* (4), 711–719.
- [33] Shan, X.; Chen, H. *Phys. Rev. E* **1993**, *47* (3), 1815–1819.
- [34] Shan, X.; Chen, H. *Phys. Rev. E* **1994**, *49* (4), 2941–2948.

- [35] Swift, M. R.; Orlandini, E.; Osborn, W. R.; Yeomans, J. M. *Phys. Rev. E* **1996**, *54* (5), 5041–5052.
- [36] Zheng, H. W.; Shu, C.; Chew, Y. T. *Journal of Computational Physics* **2006**, *218* (1), 353–371.
- [37] Gunstensen, A. K.; Rothman, D. H.; Zaleski, S.; Zanetti, G. *Phys. Rev. A* **1991**, *43* (8), 4320–4327.
- [38] Liu, H.; Valocchi, A. J.; Kang, Q. *Phys. Rev. E* **2012**, *85* (4), 046309.
- [39] Coreixas, C.; Chopard, B.; Latt, J. *Phys. Rev. E* **2019**, *100* (3), 033305.
- [40] Bhatnagar, P. L.; Gross, E. P.; Krook, M. *Phys. Rev.* **1954**, *94* (3), 511–525.
- [41] Qian, Y. H.; D’Humières, D.; Lallemand, P. *EPL* **1992**, *17* (6), 479.
- [42] D’Ortona, U.; Salin, D.; Cieplak, M.; Rybka, R. B.; Banavar, J. R. *Phys. Rev. E* **1995**, *51* (4), 3718–3728.
- [43] Wen, Z. X.; Li, Q.; Yu, Y.; Luo, K. H. *Phys. Rev. E* **2019**, *100* (2), 023301.
- [44] Reis, T.; Phillips, T. N. *J. Phys. A: Math. Theor.* **2007**, *40* (14), 4033.
- [45] Gac, J. M.; Gradoń, L. *Journal of Colloid and Interface Science* **2012**, *369* (1), 419–425.
- [46] Abdusalamov, R.; Scherdel, C.; Itskov, M.; Milow, B.; Reichenauer, G.; Rege, A. *J. Phys. Chem. B* **2021**, *125* (7), 1944–1950.
- [47] Nakanishi, K.; Kanamori, K. *J. Mater. Chem.* **2005**, *15* (35–36), 3776–3786.
- [48] Kanamori, K.; Kodera, Y.; Hayase, G.; Nakanishi, K.; Hanada, T. *Journal of Colloid and Interface Science* **2011**, *357* (2), 336–344.
- [49] Du, M.; Mao, N.; Russell, S. *J Mater Sci* **2016**, *51* (2), 719–731.
- [50] Deng, X.; Wu, L.; Deng, Y.; Huang, S.; Sun, M.; Wang, X.; Liu, Q.; Li, M.; Li, Z. *J Sol-Gel Sci Technol* **2021**, *100* (3), 477–488.
- [51] Klein, L. C. *Annual Review of Materials Research* **1985**, *15* (Volume 15.), 227–248.
- [52] Venkateswara Rao, A.; Bhagat, S. D.; Hirashima, H.; Pajonk, G. M. *Journal of Colloid and Interface Science* **2006**, *300* (1), 279–285.

The table of contents entry should be 50–60 words long and should be written in the present tense. The text should be different from the abstract text.

The numerical model, which is a combination of the model based on cellular automata, and specifically the diffusion/reaction limited aggregation with the two-phase Lattice Boltzmann method, describes the gel synthesis taking into account microscopic phase separation. The model makes it possible to determine the structural properties of the obtained gel and to describe the kinetics of its formation.

Jakub M. Gac<sup>1\*</sup>, Bartosz Nowak<sup>1</sup> and Nina H. Borzęcka<sup>1,2</sup>

### Cellular automata coupled with two-phase Lattice Boltzmann model for modelling of kinetics of formation and structure of sol-gel materials

ToC figure

